

The clustering properties of the first galaxies

Massimo Stiavelli

Space Telescope Science Institute, 3700 San Martin Dr., Baltimore MD 21218, USA

and

Michele Trenti

University of Colorado, Center for Astrophysics and Space Astronomy, 389-UCB, Boulder, CO 80309, USA

ABSTRACT

We study the clustering properties of the first galaxies formed in the Universe. We find that, due to chemical enrichment of the inter-stellar medium by isolated Population III stars formed in mini-halos at redshift $z \gtrsim 30$, the (chronologically) first galaxies are composed of metal-poor Population II stars and are highly clustered on small scales. In contrast, chemically pristine galaxies in halos with mass $M \sim 10^8 M_\odot$ may form at $z < 20$ in relatively underdense regions of the Universe. This occurs once self-enrichment by Population III in mini-halos is quenched by the build-up of an H_2 photo-dissociating radiative background in the Lyman-Werner bands. We find that these chemically pristine galaxies are spatially uncorrelated. Thus, we expect that deep fields with the James Webb Space Telescope may detect clusters of chemically enriched galaxies but individual chemically pristine objects. We predict that metal-free galaxies at $10 \lesssim z \lesssim 15$ have surface densities of about 80 per square arcmin and per unit redshift but most of them will be too faint even for JWST. However, the predicted density makes these objects interesting targets for searches behind lensing clusters.

Subject headings: cosmology: theory — early universe — galaxies: high-redshift

1. Introduction

The concept of first galaxies is not as easy to define as that of first stars and it's partly a matter of convention. A first, somewhat arbitrary, decision, is the mass scale where an object becomes a galaxy. A common convention in the context of the first galaxies is describing galaxies as those objects forming within dark halos massive enough that their gaseous content can cool by atomic hydrogen (Ly α cooling), i.e. characterized by a virial temperature greater than 10^4 K (Ricotti et al. 2008; Wise & Abel 2008; Greif et al. 2008). The advantage of this definition is that it is based on a physical process and makes galaxy formation relatively independent of the presence

of a Lyman-Werner (LW) background that could hamper the formation of Population III stars in mini-halos by photo-dissociating molecular hydrogen (Lepp & Shull 1983; Tegmark et al. 1997; Haiman et al. 1997; Machacek et al. 2003; Trenti & Stiavelli 2009; Trenti et al. 2009).

Once we have defined “galaxy” we need to define “first”. The usual assumption is that “first” refers to a chronological sequence of events, so that the first galaxies are those that formed at the earliest redshifts. It is sometimes assumed that the chronologically “first” galaxies will also be the least chemically evolved ones. In fact, these objects are most likely to form in highly clustered areas and they are also very likely to have been polluted by metals produced by Population III stars forming in mini-halos (Wise & Abel 2008; Greif et al. 2008). Thus, these chronologically first galaxies would not have a primordial chemical composition. However, we can imagine another class of galaxies that would form after a LW background is in place and would then not be polluted by stars in mini-halos (Jimenez & Haiman 2006; Trenti et al. 2009; Johnson et al. 2008). These objects could conceivably form stars out of pristine primordial gas and would then be galaxies made of Population III stars. Assuming that they can form Population III stars in significant numbers, these objects would be chemically less evolved (i.e. “younger”) despite forming later in a chronological sense.

This paper is devoted to exploring the validity of the two scenarios described above and to studying the redshift distributions and clustering properties of these two classes of objects. These quantities are relevant for planning surveys to study the first galaxies with the James Webb Space Telescope and other (future) facilities, such as thirty-meter class telescopes used for imaging behind lensing clusters.

The structure of the paper is the following. In Sec. 2 we discuss our model for galaxy formation during the Dark Ages, in Sec. 3 we present our results on star formation rates and clustering. Sec. 4 concludes with prospects for future detections and speculates on the possibility that metal-free galaxies have already been observed behind a lensing cluster by Stark et al. (2007).

2. Galaxy formation during the reionization era

Our method is based on a combination of numerical simulations and analytical considerations developed by Trenti & Stiavelli (2007), Trenti et al. (2008), Trenti & Stiavelli (2009), Trenti et al. (2009), and Trenti & Shull (2010). Here we briefly summarize the main properties of our model.

We determine the dark matter halo formation rate and merging history using either extended Press-Schechter modeling based on the Sheth & Tormen (1999) mass function (see Trenti & Stiavelli 2009) or high-resolution cosmological simulations (see Trenti et al. 2009). We populate metal-free halos with stars by taking into account the cooling timescales for atomic and molecular hydrogen, including also radiative feedback due to LW radiation (Trenti & Stiavelli 2009, see also Stiavelli 2008). The minimum halo mass required for metal-free star formation from our model is shown as solid black line in left panel of Fig. 1. Metal-free star formation transitions from mini-halos with

virial temperature $T_{vir} \sim 10^3$ K, where molecular hydrogen cooling is efficient at $z \gtrsim 30$, to more massive halos ($T_{vir} \gtrsim 10^4$ K) at $z \lesssim 15$, where Ly- α cooling is possible independently of the radiation background. The minimum mass we require for star formation is consistent with the results from detailed hydrodynamic simulations of metal free star formation in the presence of a radiative LW background (O’Shea & Norman 2008), as discussed in detail in Trenti et al. (2009). If a halo is able to cool and if $T_{vir} \sim 10^3$ K (Abel et al. 2002; Yoshida et al. 2003; O’Shea & Norman 2007), we assume it forms a single, massive Pop III star drawn from a Salpeter initial mass function (IMF) in the mass range 50-300 M_\odot . When appropriate the star explodes as a Pair Instability Supernova (PISN) (Heger & Woosley 2002; Scannapieco et al. 2003). A constant fraction of metal-free gas ($f_* \approx 5 \times 10^{-3}$) is converted into stars when Ly α cooling is possible in halos with $T_{vir} \gtrsim 10^4$ K at lower redshift. In this case, we assume a lower characteristic mass ($O(30)M_\odot$) for Population III stars (see Yoshida et al. 2006).

The transition from metal-free to metal enriched star formation happens at a critical metallicity $Z_{crit} \sim 10^{-3.5} Z_\odot$ (Bromm & Larson 2004; Smith et al. 2009) and might be as low as $Z_{crit} \sim 10^{-6} Z_\odot$ in the presence of dust (Schneider et al. 2006). A single PISN provides enough metals to trigger the transition to metal-enriched star formation in halos with $T_{vir} \sim 10^4$ K (that is with mass $M \lesssim 3 \times 10^7$ at $z \gtrsim 10$ — see left panel of Fig. 1). In fact, several studies show that these halos may even reach a metallicity well above Z_{crit} as a result of PISN enrichment (Wise & Abel 2008; Karlsson et al. 2010; Greif et al. 2010).

For metal enriched halos, we assume that a fraction $f_* \approx 5 \times 10^{-3}$ of gas is converted into stars with a Salpeter IMF in the mass range 1-100 M_\odot . In the analytical model, metal enrichment is based on a statistical approach making use of the probability that progenitors of a halo will have formed a star before the halo collapses, as described in Trenti & Stiavelli (2007). In the numerical simulations, we regularly save full snapshots of the system and use them to construct a detailed halo tree to determine whether a halo is self-enriched. Through simply counting photons we track the establishment of an average radiative background, i.e. our models do not include detailed radiative transfer.

The numerical simulations have been run using the Particle Mesh Tree Code Gadget-2 (Springel 2005). We adopt the fifth year WMAP concordance cosmology with $\Omega_\Lambda = 0.72$, $\Omega_m = 0.28$, $\Omega_b = 0.0462$, $\sigma_8 = 0.817$, $n_s = 0.96$, $h = 0.7$. We start our main simulation at redshift $z=199$ using a box with edge $7h^{-1}$ Mpc, $N=1024^3$ dark matter particles, a mass resolution of $3.4 \times 10^4 M_\odot$ and a force resolution of $0.16 h^{-1}$ kpc. Halos are identified with a friend-of-friend halo finder (Davis et al. 1985) using a linking length equal to 0.2 the mean particle separation. In addition to in situ enrichment by progenitor mini-halos, in the numerical simulations we also consider enrichment by winds which is not included in the analytical model. We assume an outflow speed of 60 km s^{-1} from halos that contain metal-enriched galaxies, that is with $T_{vir} \gtrsim 10^4$ K (see Trenti et al. 2009 for further details). The resulting wind enrichment is consistent with what is obtained using a non-cosmological Sedov-Taylor model (e.g. Eq. 8 in Tumlinson et al. 2004), namely bubble sizes of $\lesssim 150 h^{-1} \text{ kpc}$ at $z \gtrsim 6$. Gas polluted by winds in dark matter halos that have not been self-

enriched is also likely to reach a metallicity $Z \sim 10^{-3.5} Z_{\odot}$ sufficient to trigger the transition to extremely metal poor (EMP) star formation. In fact, the typical distance traveled by winds before they encounter a non-self enriched halo is of the order of $\sim 50h^{-1}\text{kpc}$, sufficient to reach the critical level of metal pollution for metal outflows originating from a dwarf galaxy (see Section 2.1 and Figure 3 in Trenti et al. 2009).

3. Results

3.1. Galaxy Formation Rate

In Fig. 2 we show, as a function of redshift, the rate of proto-galaxies forming per year and made of chemically enriched stars (marked as PopII, dashed red line) compared to that of proto-galaxies made of Population III stars (solid blue line). The figure is derived from the analytical model for galaxies with virial temperature between 10^4 and 2×10^4 K - roughly corresponding to $\lesssim 10^8 M_{\odot}$ (see left panel of Fig. 1) - and confirms our expectation that chemically enriched galaxies form at earlier redshifts than galaxies made of population III stars. The analytical model does not include the effect of enrichment by winds which will lead to $\sim 30\%$ lower numbers of pristine objects at $z \sim 10$ (see Fig. 4 in Trenti et al. 2009).

In our model, chemically enriched galaxies peak at a redshift $z \simeq 15$, while galaxies made of Population III stars peak at a redshift $z \simeq 11$. This trend is in agreement with that shown in Fig. 1 of Trenti & Stiavelli (2009) once one considers that Pop II formation in that figure was for all halos regardless of their mass while here it is limited to halos of the prescribed virial temperature. The presence of a peak at $z \sim 15$ in the enriched galaxies is due to this mass constraint.

3.2. Clustering Properties

In Fig. 1 we show an analytical estimate of the bias as a function of redshift for halos that can contain Population III stars. Clearly the bias decreases rapidly with redshift as the Population III halos become more common. However, Fig. 1 does not distinguish between halos that are polluted by winds and those that are truly metal free (self-enrichment does not influence the bias). To address the expected clustering properties of the first galaxies we need to resort to the numerical simulation results, which of course carry spatial information on the presence of neighbouring galaxies capable of polluting pockets of metal free stars. This effect is important only for redshift $z \lesssim 15$ because at higher redshift the metal outflows do not have enough time to propagate far from their host galaxies (see Trenti et al. 2009).

The cosmological simulation allows us to measure the bias for both the chemically enriched “first” galaxies population and the Population III galaxies. To quantify their clustering we use the positions of galaxy-hosting dark matter halos to construct the three dimensional two-point corre-

lation function $\theta(r)$ in comoving space, defined as the excess number of pair counts at separation r over those from a uniform random distribution. We generate a random uniform distribution of 40000 points within the simulation box and adopt the Landy & Szalay (1993) estimator:

$$1 + \theta(r) = \frac{DD(r) - 2DR(r) + RR(r)}{RR(r)}, \quad (1)$$

where $DD(r)$ are the halo-halo pair counts with distance bound in an annulus centered on r . Similarly $DR(r)$ are the halo-random pair counts and $RR(r)$ the random-random counts within the same annulus.

In Fig. 3 we show for redshift $z = 9.5$ the correlation function as a function of radius for chemically enriched protogalaxies, that is for all dark matter halos with $10^4\text{K} \leq T_{vir} \leq 2 \times 10^4$ K that had past star formation bursts (θ_{PopII} marked as "Pop II Gal", solid red) and for galaxies containing Population III stars, that is dark matter halos with $T_{vir} \geq 10^4$ K that are chemically pristine with respect to both wind and self-enrichment (θ_{PopIII} , blue line)¹. We also show the correlation function for extremely metal poor protogalaxies, at or above the critical metallicity $Z \sim 10^{-3.5} Z_{\odot}$, enriched by winds but otherwise not self-enriched, again hosted in halos with $10^4\text{K} \leq T_{vir} \leq 2 \times 10^4$ K (green line). In the same figure we also show the ratio of $\theta(r)_{PopIII}/\theta(r)_{PopII}$ to quantify the relative bias of these two galaxy populations (Porciani et al. 1999; Sheth & Tormen 1999). Clearly for radii in excess of a few tens of kpc the chemically enriched galaxies exhibit stronger clustering than the galaxies containing Population III stars. The low bias for Population III galaxies compared to their metal enriched counterparts extends up to $z \sim 15$ (see Fig. 4).

4. Discussion and Conclusions

Fig. 3 predicts that galaxies containing Population III stars will be essentially uncorrelated on scales larger than ~ 150 comoving kpc. At redshift $z = 9.5$, 1 arcsec corresponds to roughly 50 comoving kpc in the transverse direction. This implies that the typical arcmin scales of the imaging instruments on the James Webb Space Telescope correspond to a few comoving Mpc and on those scales we should not detect any significant clustering for galaxies with primordial chemical composition. In contrast, enriched protogalaxies could be very clustered on small scales, as they live in high density regions. Thus, in an ultradeep field with JWST we expect to detect individual unevolved galaxies at $z \simeq 10$, but small clusters of chemically evolved objects. From Fig. 2 we see that the rest frame rate of galaxy formation per comoving volume at $z \simeq 10$ is $\sim 2 \times 10^{-8} \text{Mpc}^{-3} \text{yr}^{-1}$ (estimating the halo formation rate from the simulations gives a similar number). Assuming that the burst of Population III stars is short lived, we expect that the galaxy will be visible as Population III galaxy only for a time of the order of the stellar lifetime (assumed to be 2×10^6 yrs).

¹There are no chemically pristine halos with $T_{vir} \geq 2 \times 10^4$ K in our simulation because we assume Population III star formation once halos are capable of Ly α cooling (Trenti et al. 2010)

Considering that the comoving volume per unit redshift at $z \sim 10$ is ~ 2000 comoving Mpc^3 over an area of one arcmin squared, we predict a surface density of ~ 80 galaxies per square arcmin and per unit redshift. However, there are large uncertainties as to the luminosity such a galaxy would have. In a deep exposure, the James Webb Space Telescope should be able to detect a young cluster with a stellar mass of $10^6 M_\odot$ ². Most of the pristine galaxies will have lower stellar masses. At a virial temperature $T = 10^4$ K at $z \sim 10$ a galaxy has a halo mass of $\sim 3.7 \times 10^7 M_\odot$ and only $\sim 6 \times 10^6 M_\odot$ in baryons. It is at this stage unclear whether the Population III stellar burst in a proto-galaxy would produce many stars and with what efficiency ϵ , but $\epsilon \gtrsim 0.15$ is unlikely in the first burst. Even if the majority of these objects will be too faint, their large number density and the expected lack of strong correlations are encouraging as they make it more likely that we could detect some of these objects through a lensing cluster. A Population III galaxy of $10^6 M_\odot$ of stars formed over a stellar lifetime forms stars at about $0.3 M_\odot \text{ yr}^{-1}$ and would have a Ly α luminosity of $\sim 3 \times 10^{42} \text{ erg s}^{-1}$ (Schaerer 2003) and a Ly α line flux at $z = 10$ of $\sim 1.9 \times 10^{-18} \text{ erg s}^{-1} \text{ cm}^{-2}$. These fluxes are close to what can be detected today in a lensing cluster after modest amplification and is in fact in agreement with some reports of detections (Stark et al. 2007).

The (chronologically) first galaxies at the same redshift and the extremely poor galaxies are instead expected to be highly correlated at least on scales of a few arcsec. Thus, to first order our models predict that one should observe small clusters of chemically evolved galaxies but only isolated primordial galaxies.

We thank the anonymous referee for comments that have helped improve the paper. MS acknowledges partial support from NASA JWST IDS grant NAG5-12458. MT acknowledges partial support from the University of Colorado Astrophysical Theory Program through grants from NASA (NNX07AG77G) and NSF (AST07-07474).

REFERENCES

- Abel, T., Bryan, G. L., & Norman, M. L. 2002, *Science*, 295, 93
- Bromm, V. & Larson, R. B. 2004, *ARA&A*, 42, 79
- Davis, M., Efstathiou, G., Frenk, C. S., White, S.D.M., 1985, *MNRAS*, 292, 371
- Greif, T. H., Johnson, J. L., Klessen, R. S., & Bromm, V. 2008, *MNRAS*, 387, 1021
- Greif, T. H., Glover, S. C. O., Bromm, V. & Klessen, R. S. 2010, *ApJ*, 716, 510
- Haiman, Z., Rees, M. J., & Loeb, A. 1997, *ApJ*, 476, 458

²In contrast, typical Lyman Break Galaxies currently found at $z > 7$ are older (stellar age $\gtrsim 100$ Myr Labbé et al. 2010) and reside in dark-matter halos with $M_{halo} \gtrsim 2 \times 10^{10} M_\odot$

- Heger, A. & Woosley, S. E. 2002, *ApJ*, 567, 532
- Karlsson, T., Johnson, J. L.; Bromm, V. 2008, *ApJ*, 679, 6
- Jimenez, R. & Haiman, Z. 2006, *Nature*, 440, 501
- Johnson, J. L., Greif, T. H., & Bromm, V. 2008, *MNRAS*, 388, 26
- Labbé, I. et al. 2010, *ApJ*, 708, 26
- Landy, S. D. & Szalay, A. S. 1993, *ApJ*, 412, 64
- Lepp, S. & Shull, J. M. 1983, *ApJ*, 270, 578
- Machacek, M. E., Bryan, G. L., & Abel, T. 2003, *MNRAS*, 338, 273
- O’Shea, B. W. & Norman, M. L. 2007, *ApJ*, 654, 66
- . 2008, *ApJ*, 673, 14
- Porciani, C., Catelan, P., & Lacey, C. 1999, *ApJ*, 513, L99
- Ricotti, M., Gnedin, N. Y., & Shull, J. M. 2008, *ApJ*, 685, 21
- Scannapieco, E., Schneider, R., & Ferrara, A. 2003, *ApJ*, 589, 35
- Schaerer, D. 2003, *A&A*, 397, 527
- Schneider, R., Omukai, K., Inoue, A. K., & Ferrara, A. 2006, *MNRAS*, 369, 1437
- Sheth, R. K. & Tormen, G. 1999, *MNRAS*, 308, 119
- Smith, B. D., Turk, M. J., Sigurdsson, S., O’Shea, B. W., & Norman, M. L. 2009, *ApJ*, 691, 441
- Springel, V., 2005, *MNRAS*, 364, 1105
- Stark, D. P., Ellis, R. S., Richard, J., Kneib, J.-P., Smith, G. P., & Santos, M. R. 2007, *ApJ*, 663, 10
- Stiavelli, M. 2008, *From First Light to Reionization: The End of the Dark Ages* (Wiley-VC)
- Tegmark, M., Silk, J., Rees, M. J., Blanchard, A., Abel, T., & Palla, F. 1997, *ApJ*, 474, 1
- Trenti, M., Santos, M. R., & Stiavelli, M. 2008, *ApJ*, 687, 1
- Trenti, M. & Shull, J.M. 2010, *ApJ*, 712, 435
- Trenti, M. & Stiavelli, M. 2007, *ApJ*, 667, 38
- . 2009, *ApJ*, 694, 879

- Trenti, M., Stiavelli, M., & Shull, M. J. 2009, *ApJ*, 700, 1672
- Trenti, M. et al. 2010, *ApJ*, 714, 202
- Tumlinson, J., Venkatesan, A., & Shull, J. M. 2004, *ApJ*, 612, 602
- Wise, J. H. & Abel, T. 2008, *ApJ*, 685, 40
- Yoshida, N., Abel, T., Hernquist, L., & Sugiyama, N. 2003, *ApJ*, 592, 645
- Yoshida, N., Omukai, K., Hernquist, L., & Abel, T. 2006, *ApJ*, 652, 6

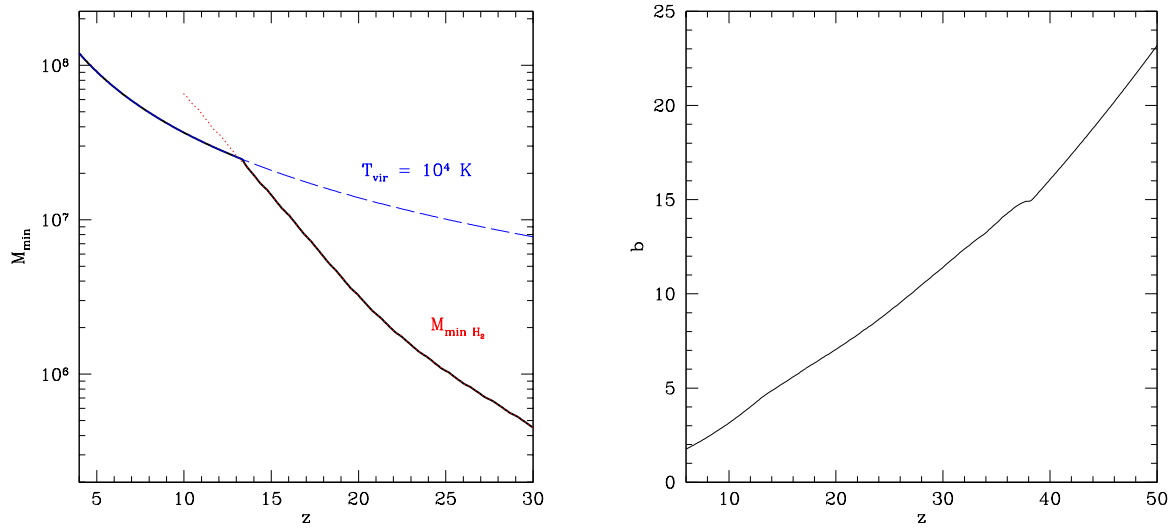


Fig. 1.— Left panel. Minimum halo mass for star formation (solid black line) required after accounting for H_2 photo-dissociation due to photons in the Lyman-Werner bands (figure from Trenti et al. 2009). At very high-redshift ($z \gtrsim 30$) the gas can cool in small mini-halos, with $T_{\text{vir}} \sim 10^3$ K. As the global star formation rate increases, H_2 cooling is suppressed and the minimum mass of a mini-halo capable of forming stars rises steadily. At $z \lesssim 15$ only halos with $T_{\text{vir}} \geq 10^4$ K can form stars. Right panel: bias for halos at the minimum mass required for star formation as shown in the left panel. The bias has been computed using the Sheth & Tormen (1999) model.

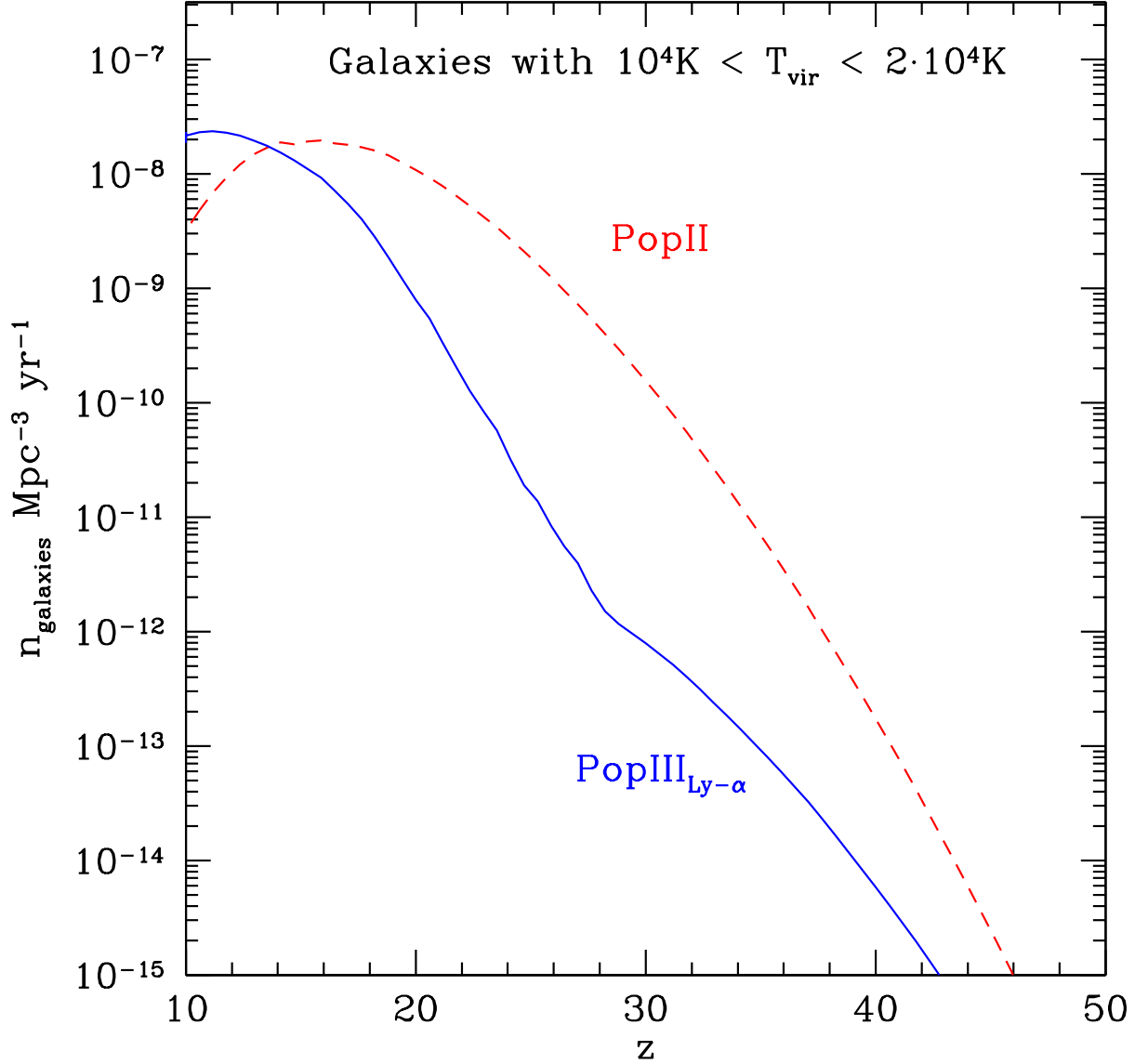


Fig. 2.— Formation rate of proto-galaxies per comoving volume (in halos with $10^4 \text{ K} \leq T_{\text{vir}} < 2 \cdot 10^4 \text{ K}$ that are either chemically pristine (solid blue line) or with a low metallicity of the order of the critical one (red dashed line). The rate (rest-frame and comoving) has been obtained from an analytical Extended Press-Schechter model (see Trenti & Stiavelli 2009) considering self-enrichment only, thus galactic metal outflows are neglected. If these were to be considered they would reduce the formation rate of PopIII proto-galaxies (see Trenti et al. 2009). The first galaxies to be formed at very high-redshift are very likely to be made of Population II (metal enriched) stars.

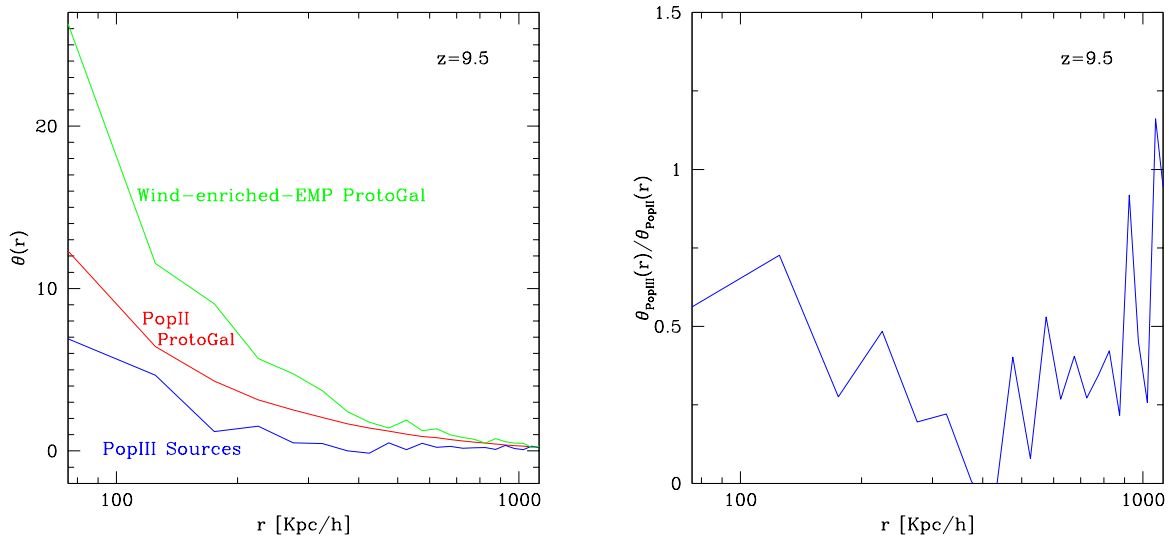


Fig. 3.— Left panel. Three-dimensional two-point correlation function for metal-free (blue) and metal-enriched (red) proto-galaxies, residing in halos with $10^4 \text{ K} \leq T_{vir} < 2 \cdot 10^4 \text{ K}$, at $z = 9.5$. We also show the correlation for extremely metal poor galaxies (green line) that have been enriched by winds. The figure has been obtained from the cosmological simulation presented in Trenti et al. (2009) and includes metal enrichment from outflows propagating at 60 km s^{-1} . Lines are an average over 9 simulation snapshots with $9 \leq z \leq 10$. Right panel: ratio of the Pop III to Pop II correlation functions, which further highlights that metal-free proto-galaxies are significantly less clustered on small scales ($r \lesssim 1 \text{ Mpc}/h$) than their metal-enriched counterparts with similar halo mass.

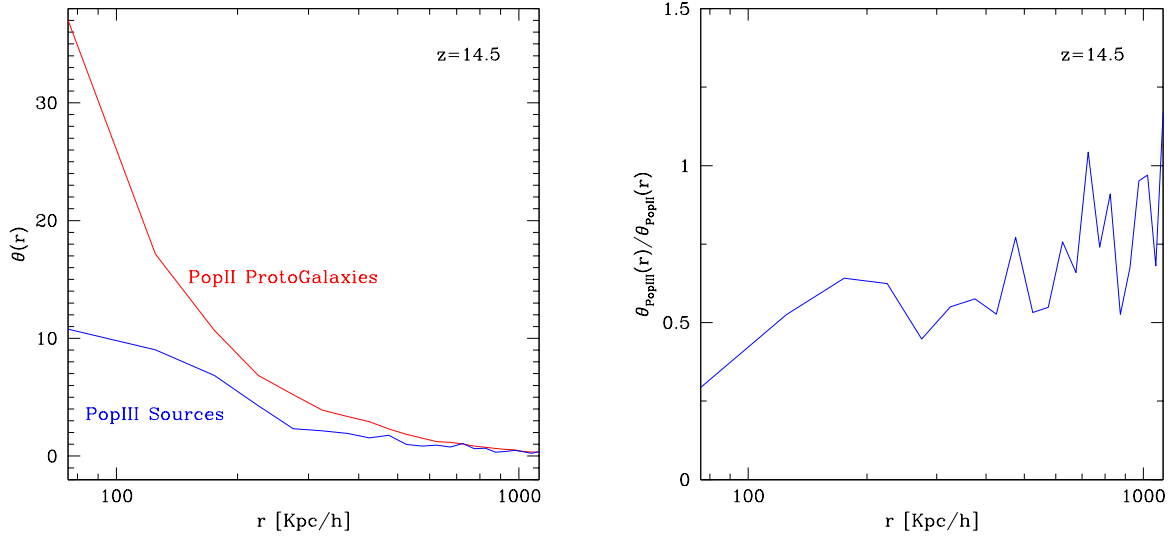


Fig. 4.— Left panel. Three-dimensional two-point correlation function for metal-free (blue) and metal-enriched (red) proto-galaxies as in Fig. 3 measured at $z = 14.5$. The figure has been obtained by averaging over 5 simulation snapshots with $14 \leq z \leq 15$. Right panel: ratio of the two-correlation functions.